*Desalination and Water Treatment*
www.deswater.com

doi: 10.1080/19443994.2015.1107756

57 (2016) 20411–20421
September

Taylor & Francis
Taylor & Francis Group

# A novel nanoadsorbent Ni/Ni$_x$B for preconcentration of arsenic(III) and arsenic(V) before hydride generation-atomic absorption spectrometric determination

Yasemin İşlek Coşkun, Tülin Deniz Çiftçi, Emür Henden*

*Faculty of Science, Department of Chemistry, University of Ege, 35100 Bornova, Izmir, Turkey, Tel. +90 232 311 2355; Fax: +90 232 388 8264; emails: yasemin.islek@ege.edu.tr (Y. İşlek Coşkun), tulin.deniz.ciftci@ege.edu.tr (T.D. Çiftçi), emur.henden@ege.edu.tr (E. Henden)*

Received 17 April 2015; Accepted 8 October 2015

**ABSTRACT**

A novel adsorbent named Ni/Ni$_x$B nanoparticles was synthesized for the preconcentration of both As(III) and As(V) from water samples. Both adsorbent preparation and adsorption procedure were optimized. The adsorption efficiencies for both As(III) and As(V) were higher than 99% when the initial pHs ranged from 4.0 to 10.0. The rate of the adsorption was high, and in the first 10 min, the adsorption efficiency reached 95%. Adsorbed As(III) and As(V) were recovered with high efficiencies from the adsorbent using 2 mol L$^{-1}$ HCl. Under the optimal conditions, an enrichment factor of 50 was reached. Hundred-fold excess of Cd$^{2+}$, Cu$^{2+}$, Mg$^{2+}$, Zn$^{2+}$, K$^{+}$, SiO$_4^{4-}$, SO$_4^{2-}$, and PO$_4^{3-}$ ions did not affect the adsorption efficiencies of As(III) and As(V). The adsorption for both As(III) and As(V) obeyed the Freundlich and Langmuir isotherms. The maximum adsorption capacities calculated from the Langmuir isotherm were 2,500 mg g$^{-1}$ for both species, and the adsorptions were favorable. The validation and the real sample application studies showed that the adsorbent was appropriate for the preconcentration of both As(III) and As(V) from water samples.

*Keywords:* Nanoparticles; Arsenic; Preconcentration; Hydride generation; Atomic absorption spectrometry

## 1. Introduction

A ubiquitous toxic element arsenic is naturally present in the environment. It exists as inorganic arsenic species (arsenite AsO$_3^{3-}$ and arsenate AsO$_4^{3-}$) and organic arsenic species, such as monomethylarsonate (MMA), dimethylarsonate (DMA), arsenobetaine (AsB), and arsenocholine (AsC) [1]. Arsenic has four oxidation states: As(V), As(III), As(0), and As(−III). The oxidation state and the chemical form of arsenic are responsible for its mobility and toxicity [2]. It is reported that As(III) and its inorganic species are more toxic than As(V) and their organic arsenic compounds [3].

Arsenic is related to severe health effects such as dermal changes, respiratory, cardiovascular, gastrointestinal, genotoxic, and mutagenic, carcinogenic effects. Food and water are the primary source of arsenic to humans. A maximum contaminant level in potable water supplies is recommended at 10 μg L$^{-1}$ by WHO [4]. Biological tissues and fluids generally contain organic arsenic species, while inorganic

---

*Corresponding author.

arsenic is found in the environmental waters, soils, and sediments.

The majority of available techniques are not sensitive enough to detect concentrations of arsenic as is; therefore, a preconcentration step becomes a necessity [5]. Moreover, the preconcentration techniques separate analyte from most of the matrix components. Preconcentration techniques based on the sorption of analyte on solids have commonly been used. Analyte is recovered from the solid by elution using a suitable eluent and, subsequently, the preconcentrated analyte is determined. Nanoparticles are attractive sorbent materials for preconcentration because of low temperature modification, large specific surface area, and high sorption capacity [6]. There are a lot of studies about arsenic preconcentration and removal with nanoscaled particles in the literature. Wang et al. have removed arsenic species from real underground water using newly synthesized magnetic nanoparticles impregnated chitosan beads (MICB) as an adsorbent [7]. Montmorillonite-supported nanoscale zero-valent iron (Mt-nZVI) was synthesized to remove inorganic arsenic (As) from aqueous solutions [8]. Removal of arsenic species in contaminated natural water by hydrous cerium oxide nanoparticles was also reported [9]. For the removal of arsenic ions from water samples, ultrafine iron oxide ($\alpha$-$Fe_2O_3$) nanoparticles were also synthesized [10]. Erdoğan et al. preconcentrated and separated arsenic species using nano zirconium dioxide–boron oxide ($ZrO_2/B_2O_3$) composite material [11]. Ionically modified magnetic adsorbent was also used for the removal of As(V) [12]. Deng et al. have applied aluminum hydroxide gel for the direct enrichment and separation of trace amount of arsenic from water samples [13].

It is known that the transition metal ions, particularly nickel, interfere severely in the determination of hydride-forming elements in atomic spectroscopy when a hydride generation technique (HG) is used. This interference has commonly been attributed to the sorption or decomposition of the arsine and the other volatile analyte hydrides by the black precipitate formed when Ni(II) reacted with $NaBH_4$. However, Henden et al. elucidated that the particles formed by reacting Ni(II) with $NaBH_4$ adsorb As(III) and As(V) species before the reduction reaction rather than adsorbing or decomposing arsine. The black particles were identified as the mixture of nickel and nickel boride nanoparticles [14].

Çiftçi and Henden have recently reported the application of nano nickel- /nickel boride-coated resin for the column removal of arsenic from water [15]. According to the literature survey, nickel/nickel boride nanoparticles have so far not been used for the preconcentration purposes. Therefore, the aim of this work was to develop a novel preconcentration method for trace arsenic determination in water using nickel/nickel boride ($Ni/Ni_xB$) nanoparticles as an adsorbent. The effects of various parameters such as pH, sample volume, and contact time were investigated, and the method development was applied successfully to various water and mineral water samples.

## 2. Materials and methods

### 2.1. Apparatus

A GBC Model 904 PBT atomic absorption spectrometer was used for the determination of arsenic. A quartz tube atomizer, a laboratory-made batch-type hydride generation system [16] and GBC Model HG3000 continuous flow hydride generator were employed. An arsenic hollow cathode lamp operated at 8.0 mA and a spectral band width of 1.0 nm, and 193.7 nm arsenic line were employed. Quantification was based on peak area.

### 2.2. Reagents and materials

All chemicals used for the experiments were of analytical reagent grade. Distilled water was used for dilutions of the solutions. Laboratory glassware was kept overnight in a 10% (v/v) $HNO_3$ solution and then rinsed with distilled water.

Stock solutions of As(III) and As(V) at a concentration of 1,000 mg $L^{-1}$ were prepared by dissolving $As_2O_3$ (Merck) and $Na_2HAsO_4{\cdot}7H_2O$ (Merck), respectively, in concentrated HCl and diluting with distilled water. Stock solutions contained 2 mol $L^{-1}$ HCl. The calibration graph was drawn using the standard solutions prepared daily by dilution of the stock solutions. Cu(II), Au(III), and Ni(II) solutions were prepared from $CuSO_4$ anhydride (Merck), metallic gold (99.999% pure), and $Ni(NO_3)_2{\cdot}6H_2O$ (Merck), respectively. $NaBH_4$ solutions at 0.6 and 4% (w/v) were prepared by dissolving the powder (Merck, 99% pure) in 0.15 and 0.05 mol $L^{-1}$ NaOH solutions, respectively. Potassium iodide (KI) (Merck) and EDTA (Merck) solutions were prepared by dissolving in distilled water.

### 2.3. Analytical procedure for the determination of As(III) and As(V)

The operating conditions used for As(III) and As(V) determinations were listed earlier [17]. As(V) was reduced to As(III) before the generation of arsine with

$NaBH_4$. For this purpose, 1 mL of concentrated HCl and 2 mL of 50% KI were added to 9 mL of the sample solution. The final solution contained 8.3% KI and 1 mol $L^{-1}$ HCl. The solution was kept aside for 15 min for the reduction of As(V) to As(III), and, then appropriate amount of ascorbic acid was added into the solution to reduce $I_2$ formed.

Continuous flow hydride generator system was employed for the determination of total arsenic (As (III) + As(V)) after the KI reduction procedure. To generate arsine, 0.6% (w/v) sodium tetrahydroborate(III), 10.2 mol $L^{-1}$ HCl, and sample solutions were pumped into a mixing manifold at flow rates of 2.0, 2.0, and 8.0 mL $min^{-1}$, respectively. Arsine gas generated was separated from the solution in a gas–liquid separator and swept to the quartz tube atomizer with a nitrogen flow for AAS measurement.

For the determination of As(III) and, after the prereduction step with KI, As(V) species with the batch system, the concentrations of HCl in sample and standard solutions were 0.1 mol $L^{-1}$. Solution of 1 mL of 4% $NaBH_4$ was injected into the reaction vessel containing 1.0 mL of sample or standard solutions and 0.25 mL of 0.2 mol $L^{-1}$ EDTA. Arsine gas was swept by nitrogen flow through a $CaCl_2$ and $CaSO_4$ containing drying tube into the quartz tube atomizer for AAS measurements.

### 2.4. Preparation of the adsorbents

The adsorbents obtained from Cu(II) and Au(III) were prepared under air atmosphere. $Ni/Ni_xB$ nanoparticles were prepared under air and also nitrogen atmosphere.

#### 2.4.1. Under air atmosphere

Under air atmosphere, 25 mL of 2.5% (w/v) of Ni (II) solution in 0.1 mol $L^{-1}$ HCl was added into a beaker and, while stirring on a magnetic stirrer, 25 mL of 4% $NaBH_4$ was added in nine minutes using a burette. Black precipitate immediately appeared after the first drop of sodium borohydride solution. The mixture was allowed to stand until gas bubbles disappeared. Afterward, the mixture was put in a polyethlylene bottle and shaken in a water bath at 25˚C for 30 min to obtain fine particles. Ultra centrifugation technique was used to separate the black $Ni/Ni_xB$ nanoparticles from the liquid phase. Particles were washed and centrifuged at least three times with 20 mL portions of distilled water and then with acetone to remove the remaining water. Prepared $Ni/Ni_xB$ nanoparticles were finally dried in a water bath at 75˚C for two hours under nitrogen atmosphere.

Nanoparticles of copper were prepared using 500 mg $L^{-1}$ Cu(II) solution based on the same procedure. Gold-coated silica particles were prepared by reduction with $NaBH_4$ according to the literature [18].

#### 2.4.2. Under nitrogen atmosphere

Three holes were made on the lid of a 100-mL polyethylene bottle. The first hole was for nitrogen gas inlet, second one was for $NaBH_4$ flow, and the last one was for gas outlet. Then, 25 mL of 2.5% (w/v) of Ni(II) was added to the bottle. While Ni(II) solution was stirred on a magnetic stirrer under $N_2$ atmosphere, 25 mL of 4% (w/v) $NaBH_4$ was added in nine minutes using a burette. The black precipitate formed was separated from the liquid phase by ultracentrifugation technique. Particles formed were then washed, centrifuged, and dried as described above.

### 2.5. Adsorption studies

Nanoparticles were prepared from Ni(II) solution under air atmosphere, unless otherwise stated for adsorption experiments. As(III) and As(V) solutions at pH ~6 were added on 10 mg of the adsorbents and shaken in a water bath at 25˚C for an hour. After the adsorption, the solutions were separated from the adsorbent by centrifugation. Unadsorbed As(III) and As(V) were determined in the supernatant solution.

Adsorption process was quantified by calculating the adsorption efficiency (%) as defined by the following equation:

$$\text{Adsorption efficiency } (\%) = \frac{(C_o - C_e)}{C_o} \times 100 \quad (1)$$

where $C_o$ is the initial concentration and $C_e$ is the equilibrium concentration, μg $L^{-1}$. The amount of arsenic adsorbed per unit mass of the adsorbent (adsorption capacity), g $g^{-1}$, is evaluated using the following equation:

$$\text{Adsorption capacity } (\text{g g}^{-1}) = \frac{(C_1 - C_2)}{w} \times V \quad (2)$$

where $C_1$ is the initial concentration and $C_2$ is the equilibrium concentration (g $L^{-1}$), $w$ is the amount of the adsorbent (g), and $V$ is the volume of arsenic solution (L).

## 3. Results and discussions

In order to obtain the highest arsenic adsorption capacity and efficiency, some optimization studies were done. Optimum concentration of Ni(II) for the preparation of the adsorbent, and its preparation condition (under air or nitrogen atmosphere), reduction time of Ni(II) with $NaBH_4$, adsorption pH, contact time of the adsorbent with arsenic solution, and sample volume were optimized. Also, nanoparticles were obtained from different metal ions for comparison.

### 3.1. Optimization studies for the preparation of the adsorbent

#### 3.1.1. Choice of metal ion for adsorbent preparation under air atmosphere

Three metal ions (Cu(II), Au(III), and Ni(II)) were investigated in order to obtain most effective nanoparticles for arsenic adsorption. While copper and nickel nanoparticles were prepared using 500 mg $L^{-1}$ solutions of Cu(II) and Ni(II) as described above, silica-coated gold nanoparticles were prepared according to the literature [18]. The nanoparticles formed were used for arsenic adsorption. For the adsorption studies, 10 mL of 50 mg $L^{-1}$ As(III) and As(V) solutions were added onto 10 mg of the nanoparticles. The most effective arsenic adsorption (>99.5%) was obtained with the nanoparticles prepared from Ni(II). While gold nanoparticles did not adsorb the arsenic species significantly, copper nanoparticles adsorbed As(III) and As(V), by 15 and 21%, respectively. Therefore, Ni (II) was chosen as the metal ion for the preparation of the nanoadsorbent.

#### 3.1.2. Choice of the adsorbent preparation conditions

Arsenic adsorption efficiencies of the adsorbents prepared under air and nitrogen atmosphere were determined. Arsenic solutions (50 mL) at concentrations of 1,000 μg $L^{-1}$ were added onto 10 mg adsorbents. Adsorption efficiencies were 96% for As(III) and 95% for As(V) using the adsorbent prepared under nitrogen atmosphere. However, 99% and higher adsorption efficiencies were obtained for both As(III) and As(V) using the adsorbent prepared under air atmosphere, and therefore, air atmosphere has been used in the further studies.

#### 3.1.3. The effect of reduction time of Ni(II) with $NaBH_4$ while preparing the adsorbent

Although the reaction of Ni(II) with $NaBH_4$ is very fast, the contact time of the black precipitate formed with the excess $NaBH_4$ might result in the variation of the precipitate surface which may in turn affect the adsorption process. Therefore, the effect of the reduction time of Ni(II) with excess $NaBH_4$ on arsenic adsorption efficiency was studied. For this purpose, 2 mL of 4% $NaBH_4$ solution was added onto 10 mL of 0.1% Ni(II) solution and the mixture was shaken for 5–180 min at 25℃. Adsorbent containing 10 mg nickel thus prepared was used for adsorption of 20 mL of 1,000 μg $L^{-1}$ As (III) solution at pH ~6. The results show that the arsenic adsorption efficiencies were all higher than 95%, and the contact time of Ni(II) with $NaBH_4$ is not a significant parameter. However, shaking is necessary to avoid excess aggregation of the adsorbent and obtain finer particles. Therefore, the reduction time was chosen as 30 min.

### 3.2. Characterization studies

Characterization of the adsorbent was performed using techniques such as scanning electron microscopy and energy dispersive X-ray spectrometry, X-ray diffraction, X-ray photoelectron spectroscopy, thermogravimetric analysis, and elemental analysis. The results of characterization studies were defined earlier in detail. The structure of the adsorbent was suggested as $Ni_xB$ and Ni(0), and also $Ni(OH)_2$ possibly formed on the particles surface. $Ni(OH)_2$ and Ni(0) thus prepared were reported to have failed to adsorb As(III), As(V), and arsine significantly [14].

### 3.3. The effect of the adsorbent dose

Different adsorbent doses 0.25–5.0 g $L^{-1}$ were used for 10 mL of 100 μg $L^{-1}$ As(III) adsorption. High adsorption efficiencies were observed for all the selected adsorbent doses (Table 1).

Table 1
The effect of adsorbent dose on arsenic adsorption efficieny (arsenic solution; 10 mL, 100 μg $L^{-1}$ As(III))

| Adsorbent dose (g $L^{-1}$) | Arsenic adsorption efficiency (%) |
|---|---|
| 0.25 | 99.0 |
| 0.5 | >99.5 |
| 1.0 | >99.5 |
| 2.0 | >99.5 |
| 3.0 | >99.5 |
| 5.0 | >99.5 |

### 3.4. The effect of initial pH on the arsenic adsorption efficiency

It is important to find out the optimal pH for the adsorption studies. The pH meter was calibrated with pH 4.0, 7.0, and 10.0 buffers before all series of measurements. The pH of 25 mL of 100 µg $L^{-1}$ As(III) solutions were adjusted to 4.0, 5.0, 6.0, 7.0, 8.0, 9.0, and 10.0 using HCl or NaOH solutions, and each solution was added onto 10 mg adsorbent. After the separation of liquid and solid phases, arsenic remaining in the solution was analyzed. According to Fig. 1, there was no significant change in the adsorption efficiencies for the selected pH intervals. The adsorption efficiencies were higher than 99% for all the initial pHs used.

In order to investigate the effect of the contact time of the adsorbent with the solutions, As(III) solution at pH ~6 and, in parallel, distilled water were added on $Ni/Ni_xB$ nanoparticles. pH values of the solutions were measured by time. The results are shown in Fig. 1 (inserted figure). It was seen that pH values of distilled water reached ~9 in the first minute. Similar equilibrium pH values were obtained using As(III) solutions with initial pH between 4 and 10. These results explain why the variations in the initial solution pH did not significantly affect arsenic adsorption efficiencies.

### 3.5. The effect of contact time on arsenic adsorption efficiency

A 25 mL of As(III) solution (50 µg $L^{-1)}$ at pH ~6 was added on to 10 mg of the adsorbent and shaken at 25˚C for various durations (1–120 min). The remaining arsenic in the solutions was determined. The adsorption rate was very high, and adsorption efficiency reached 95% in 10 min (Fig. 2). One hour was selected as the optimal contact time.

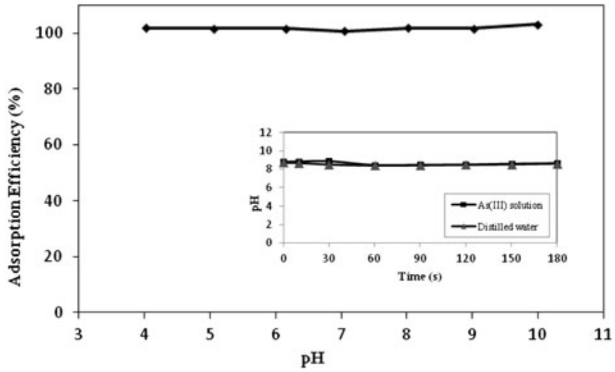

Fig. 1. The effect of initial pH on arsenic adsorption efficiency (25 mL of 100 µg $L^{-1}$ As(III) added on 10 mg adsorbent at 25˚C). Inserted figure; the effect of contact time on pH (25 mL of distilled water and 100 µg $L^{-1}$ As(III) solution at pH ~6 added on 10 mg adsorbent at 25˚C).

### 3.6. The effect of sample volume

The effect of the sample volume on the As(III) adsorption was studied in 25–250 mL range. Solutions containing 400 ng As(III) (pH ~6) at different volumes were added on 10 mg adsorbents. It was observed that the adsorption efficiencies were not affected significantly by the sample volumes. The adsorption efficiencies were about 100%.

### 3.7. Studies on the recovery of arsenic from the adsorbent

Arsenic recoveries from the adsorbent were investigated using 0.1 mol $L^{-1}$ EDTA, a mixture of 2% (w/v) NaOH and 3% (w/v) NaCl, 1 mol $L^{-1}$ $HNO_3$, 1 mol $L^{-1}$ $HNO_3$ + 10% sulfamic acid, and 2 mol $L^{-1}$ HCl. Initially, 25 mL of 1,000 µg $L^{-1}$ As(III) solution was added to 10 mg adsorbent and shaken for an hour. Then, the adsorbent with the sorbed arsenic was separated by centrifugation. The arsenic adsorption efficiency was higher than 99%. Then, arsenic-containing adsorbents were treated with the above-mentioned reagents one by one, and arsenic determinations were done in the solutions obtained. Details and results are described below.

For the recovery studies with EDTA, 5 mL of 0.1 mol $L^{-1}$ EDTA was added to the arsenic adsorbed adsorbent and heated. It was observed that most of the adsorbent was dissolved, and a blue colored solution was formed. The undissolved part of adsorbent was left in centrifuge tube. This result may show that major component of the adsorbent is a nickel-contain-

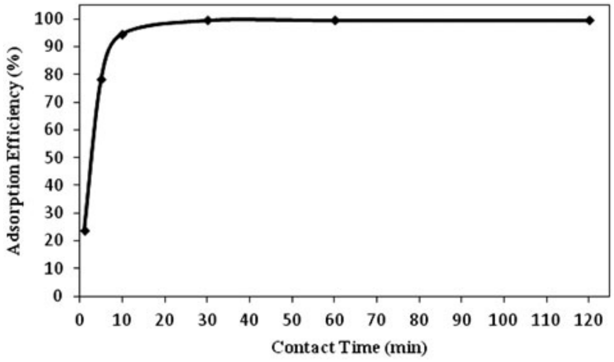

Fig. 2. The effect of contact time on arsenic adsorption (25 mL of 50 µg $L^{-1}$ As(III) added on 10 mg adsorbent at 25˚C).

ing compound or at least some of the adsorbent is elemental nickel or with a less probability a nickel compound that cannot be dissolved in EDTA. Arsenic recovery efficiencies were found as 92% for As(III) and 90% for As(V). The lack of the efficiency is probably because of some of the arsenic being held by the undissolved adsorbent.

According to Çiftçi et al., arsenic could be desorbed quantitatively from ferric hydroxide supported on silica gel (FHSS) using a mixture of 2% (w/v) NaOH and 3% (w/v) NaCl without decomposing the sorbent [17]. Therefore, in this study, the adsorbed arsenic was also attempted to be eluted three times with 5 mL of this mixture. The analysis of the solutions showed that no significant arsenic could be recovered from the Ni/$Ni_xB$ adsorbent using this mixture.

For complete recovery of arsenic from the adsorbent, the adsorbent with arsenic was dissolved in a beaker containing 5 mL of 1 mol $L^{-1}$ $HNO_3$ by heating on a hot plate for a few minutes. The concentration of arsenic measured in the solution was found to be much higher than the expected value. de Moraes Flores et al. reported that the dissolved nitrogen oxides formed during digestion with $HNO_3$ may have an important influence on the absorbance signals [19]. Therefore, 1 mL of 10% (w/v) sulfamic acid was added onto the solution and heated at 55°C for 30 min. It was observed that $NO_x$ interference was effectively eliminated with sulfamic acid and the recovery was found as 92%.

Finally, 5 mL portions of HCl solutions of different concentrations (0.05, 0.1, 0.5, 1, and 2 mol $L^{-1}$) were added on arsenic adsorbed adsorbents and the vessels were put in a water bath. Ni/$Ni_xB$ nanoparticles were dissolved in all these solutions. The arsenic measurement results showed that the recovery values were not affected by HCl concentrations significantly, and with 2 mol $L^{-1}$ HCl, the recovery value was 104.3 ± 6.18% ($n = 10$). Because of the shortest dissolution time of about ten minutes, 2 mol $L^{-1}$ HCl was used for dissolution of the adsorbent for arsenic recovery in the following experiments.

### 3.8. Enrichment factor

Another important value, enrichment factor, was determined for Ni/$Ni_xB$ nanoparticles. For this purpose, 500 mL of 0.5 μg $L^{-1}$ As(III) solution was added on 10 mg adsorbent. After adsorption for an hour, Ni/$Ni_xB$ nanoparticles containing the adsorbed arsenic was separated and dissolved in 5 mL of 2 mol $L^{-1}$ HCl and diluted to 10 mL for arsenic determination. The recovery was 100.0%. Arsenic was thus preconcentrated by 50 times.

### 3.9. Interference studies

To investigate the effect of diverse ions, 25 mL solution containing 50 μg of diverse ions ($Cd^{2+}$, $Cu^{2+}$, $Mg^{2+}$, $Zn^{2+}$, $K^+$, $SiO_4^{4-}$, $SO_4^{2-}$, and $PO_4^{3-}$) and 500 ng As(III) was added on 10 mg Ni/$Ni_xB$ nanoparticles. After shaking the solution for an hour, the adsorbent and liquid phases were separated by centrifugation. The adsorbents were dissolved in 5 mL, 2 mol $L^{-1}$ HCl and the solution was diluted to 10 mL. By measuring the unadsorbed and adsorbed arsenic, it was found that the adsorption efficiencies were more than 99% and no significant interferences were observed on the arsenic determination in the presence of 100 fold excess of the possible interfering ions.

### 3.10. Adsorption isotherms

Freundlich, Langmuir, and Dubinin–Radushkevich (D–R) isotherm models were evaluated for the determinations of maximum arsenic adsorption on Ni/$Ni_xB$.

For this purpose, 20 mL of various concentrations of As(III) and As(V) solutions (50–4,000 mg $L^{-1}$) were added onto 10 mg adsorbent and shaken for 2 h at 25°C. After the adsorption, the arsenic concentration in the remaining solution was measured.

The Freundlich equation:

$$\log q = \log k + n \log C \tag{3}$$

where $q$ is the amount adsorbed at equilibrium (mg $g^{-1}$), $k$ and $n$ is the temperature-dependent constants and $C$ is the equilibrium concentration (mg $L^{-1}$).

The Freundlich isotherm constants $k$ and $n$ found from Fig. 3 representing the adsorption capacity (mg $g^{-1}$) and intensity of the adsorbent are shown in Table 2.

Langmuir equation is applied to the experimental data for the quantification of the adsorption capacity of Ni/$Ni_xB$. Langmuir adsorption isotherm can be written as follows:

The Langmuir equation:

$$\frac{C}{q} = \frac{1}{Q_{\max} b} + \frac{C}{Q_{\max}} \tag{4}$$

where $C$ is the equilibrium concentration (mg $L^{-1}$), $q$ is the amount adsorbed at equilibrium (mg $g^{-1}$), $Q_{\max}$ is the Langmuir constant related to the capacity (mg $g^{-1}$), and $b$ is the Langmuir constant related to the energy of adsorption (L $mg^{-1}$).

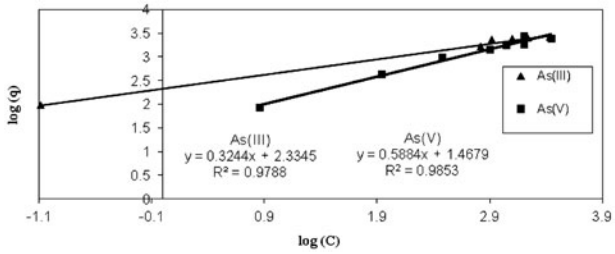

Fig. 3. Freundlich isotherm plots for the adsorption of As (III) and As(V) on Ni/Ni$_x$B (20 mL of 50, 300, 800, 1,500, 2,000, 2,500, 3,000, 4,000 mg L$^{-1}$ As(III) and As(V) solution added on 10 mg adsorbent at 25˚C).

The amount adsorbed at equilibrium ($q$) vs. the initial concentration ($C_o$) is shown in Fig. 4. The values of $Q_{\max}$ and $b$ were calculated from the slope and the intercept of the linear plots $C/q$ vs. $C$ (Fig. 5) shown in Table 2.

By considering higher $R^2$ values, it can be concluded that the Freundlich isotherm model is better fitted the equilibrium for As(V) and As(III). Table 3 shows the capacities of various adsorbents used for arsenic adsorption in the literature for comparison. It can be seen that Ni/Ni$_x$B nanoparticles have incomparably high arsenic adsorption capacity (2,500 mg g$^{-1}$ for both As(III) and As(V)) compared with that in the literature.

The dimensionless equilibrium parameter $R_L$ was determined using the following equation in order to predict the adsorption efficiency of the adsorption process:

$$R_L = \frac{1}{1 + bC_o} \tag{5}$$

where $C_o$ is the initial concentration.

Values of $R_L < 1$ represent favorable adsorption, whereas values greater than 1 represent unfavorable adsorption. The $R_L$ values for the various initial concentrations are shown in Fig. 6. The values obtained show that our system is favorable.

The equilibrium data were also fitted to the D–R isotherm model to determine the nature of adsorption processes as physical or chemical.

$$\ln Q = \ln Q_m - k\varepsilon^2 \tag{6}$$

where $\varepsilon$ (Polanyi potential) = $[RT \ln(1 + (1/C_e)]$, $Q$ is the amount of As(III) adsorbed per unit weight of adsorbent (mol g$^{-1}$), $Q_m$ is the adsorption capacity (mol g$^{-1}$), $C_e$ is the equilibrium concentration (mol L$^{-1}$) of As(III) in aqueous solution, $k$ is a constant related to adsorption energy, $R$ is the gas constant and $T$ is the temperature (K).

DR isotherm constants $k$ and $Q_m$ were calculated from the slope and intercept of the plot (Fig. 7) shown in Table 2.

The mean free energy of adsorption ($E$), defined as the free energy change when one mole of ion is transferred to the surface of the solid from infinity in solution, can be calculated from the $k$ value using the equation:

Table 2
Constant values of Freundlich, Langmuir, and D–R isotherm

| | Related equation | As(III) | As(V) |
|---|---|---|---|
| Freundlich isotherm | | | |
| $n$ | $\log q = \log k + n \log C$ | 0.3244 | 0.5884 |
| $K$ | | 216.0 | 29.37 |
| $R^2$ | | 0.9788 | 0.9853 |
| Langmuir isotherm | | | |
| $Q_{\max}$ (mg g$^{-1}$) | $\frac{C}{q} = \frac{1}{Q_{\max}b} + \frac{C}{Q_{\max}}$ | 2,500 | 2,500 |
| $b$ (L mg$^{-1}$) | | 0.003241 | 0.002167 |
| $R^2$ | | 0.9521 | 0.9604 |
| D–R isotherm | | | |
| $E$ (kJ mol$^{-1}$) | $\ln Q = \ln Q_m - k\varepsilon^2$ | 0.39 | 0.44 |
| $Q_m$ (g g$^{-1}$) | | 2.585 | 2.139 |
| $Q_m$ (mol g$^{-1}$) | | 0.0345 | 0.0286 |
| $K$ (mol$^2$ kJ$^{-2}$) | | 3.3269 | 2.5935 |
| $R^2$ | | 0.9375 | 0.9018 |

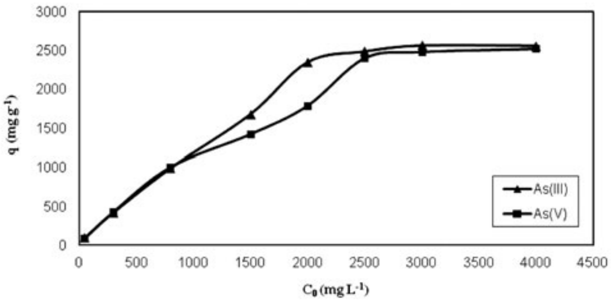

Fig. 4. The amount adsorbed at equilibrium ($q$) vs. the initial concentration ($C_0$) for the adsorption of As(III) and As(V) on Ni/Ni$_x$B (20 mL of 50, 300, 800, 1,500, 2,000, 2,500, 3,000, 4,000 mg L$^{-1}$ As(III) and As(V) solution added on 10 mg adsorbent at 25˚C).

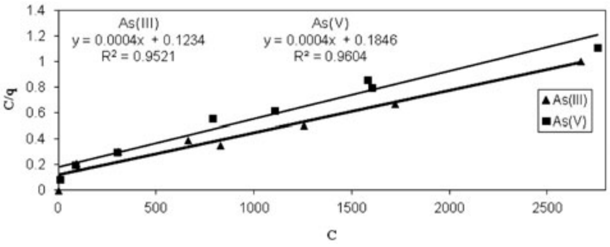

Fig. 5. Langmuir isotherm plots for the adsorption of As(III) and As(V) on Ni/Ni$_x$B (20 mL of 50, 300, 800, 1,500, 2,000, 2,500, 3,000, 4,000 mg L$^{-1}$ As(III) and As(V) solution added on 10 mg adsorbent at 25˚C).

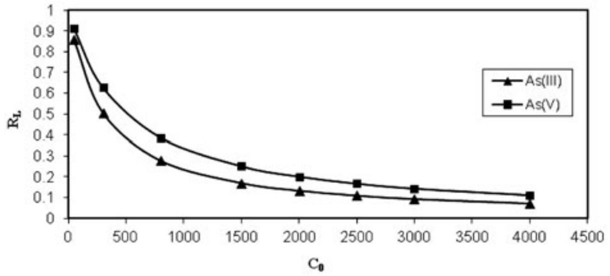

Fig. 6. The $R_L$ values vs. various initial As(III) and As(V) concentrations.

$$E = (-2k)^{-0.5} \tag{7}$$

The adsorption type can be estimated from the magnitude of E. If the value is between 8 and 16 kJ mol$^{-1}$, the adsorption type can be explained by ion exchange. However, if the values of $E$ are below 8 kJ mol$^{-1}$ the adsorption type can be explained by physical process. As seen from the Table 2, $E$ values were calculated as 0.39 kJ mol$^{-1}$ for As(III) and 0.44 kJ mol$^{-1}$ for As(V). $E$ values for both As(III) and As(V) are <8 kJ mol$^{-1}$ showing the type of the adsorption as physical.

### 3.11. Analytical figures of merit

Linear calibration graphs were drawn in the range of 5–20 μg L$^{-1}$ As(III) for the continuous flow system.

Table 3
Arsenic adsorption capacities and efficiencies of some adsorbents

| Nanoparticles | Arsenic(III) Capacity (mg g$^{-1}$) | Arsenic(III) Efficiency (%) | Arsenic (V) Capacity (mg g$^{-1}$) | Arsenic (V) Efficiency (%) | Enrichment factor | Refs. |
|---|---|---|---|---|---|---|
| Zero-valent iron (ZVI) | 18.2 | ~100 | 12.0 | ~100 | – | [20] |
| Cupric oxide (CuO) | 26.9 | 90 | 22.6 | 99 | – | [21] |
| Palladium nanoparticles | 4 | 100 | 1 | 100 | 50 | [22] |
| $ZrO_2/B_2O_3$ | – | <5 | 98.04 | ~100 | 20 | [11] |
| α-$Fe_2O_3$ | 95 | ~100 | 47 | ~100 | – | [10] |
| Hydrous cerium oxide(HCO) | 170 | >99 | 107 | >99 | | [9] |
| Ionically modified magnetic nanoparticles (PPhSi-MNPs) | – | – | 50.5 | 97 | | [12] |
| Montmorillonite-supported nanoscale zero-valent iron (Mt-nZVI) | 59.9 | – | 45.5 | | | [8] |
| Magnetic nanoparticles impregnated chitosan beads (MICB) | 35.3 | 97.9 | 35.7 | 99.5 | | [7] |
| Ni/Ni$_x$B | 2,500 | >99.5 | 2,500 | >99.5 | 50 | Present work |

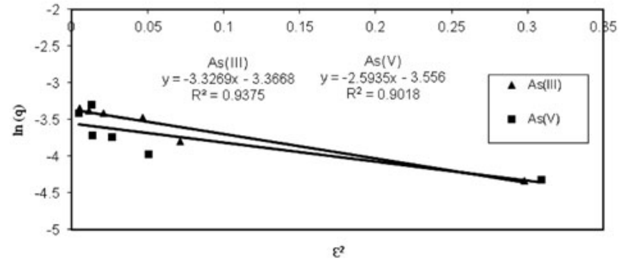

Fig. 7. D–R isotherm plots for the adsorption of As(III) and As(V) on Ni/Ni$_x$B (20 mL of 50, 300, 800, 1,500, 2,000, 2,500, 3,000, 4,000 mg L$^{-1}$ As(III) and As(V) solution added on 10 mg adsorbent at 25˚C).

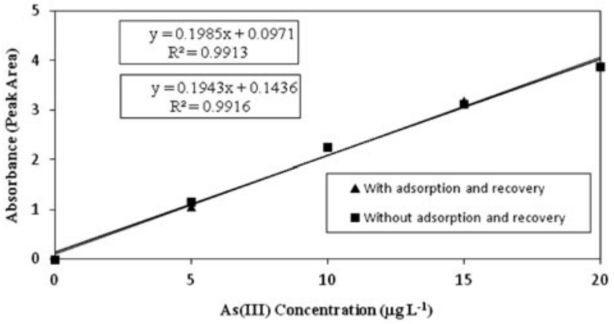

Fig. 8. Typical regression line between absorbance and arsenic concentration with and without employing the adsorption and recovery procedures (50 mL of As (III) standard solutions were added on 10 mg Ni adsorbents and the adsorbent was dissolved with 5 mL 2 M HCl).

Table 4
Determination of total arsenic in certified reference material and in some natural water samples (*n*: 3, CRM: EnviroMAT drinking water-low, certified value for total arsenic 0.010 mg L$^{-1}$)

| | | Added (μg L$^{-1}$) | | Found (μg L$^{-1}$) | | Recovery (%) | |
|---|---|---|---|---|---|---|---|
| Samples | Certified value (mg L$^{-1}$) | As(III) | As(V) | Total As | | Total As | |
| CRM | 0.010 | – | – | 0.0099 ± 0.0003 | | 99.0 | |
| Bottled water | | – | – | BLD | – | – | – |
| | | 5 | – | 5.39 ± 0.13 | – | 107.8 | – |
| | | – | 5 | – | 5.52 ± 0.075 | – | 110.4 |
| | | 10 | – | 10.90 ± 0.31 | – | 109.0 | – |
| | | – | 10 | – | 11.21 ± 0.32 | – | 112.1 |
| Tap water | | – | – | 4.60 ± 0.70 | – | – | – |
| | | 5 | – | 9.86 ± 0.84 | – | 105.2 | – |
| | | – | 5 | – | 9.70 ± 1.02 | – | 102.0 |
| | | 10 | – | 15.27 ± 1.16 | – | 106.7 | – |
| | | – | 10 | – | 14.69 ± 0.82 | – | 100.9 |
| Mineral water 1 | | – | – | 8.67 ± 0.51 | – | – | – |
| | | 5 | – | 13.65 ± 0.56 | – | 99.4 | – |
| | | – | 5 | – | 13.94 ± 0.54 | – | 105.4 |
| | | 10 | – | 18.71 ± 0.35 | – | 100.4 | – |
| | | – | 10 | – | 18.72 ± 0.40 | – | 100.5 |
| Mineral water 2 | | – | – | 2.98 ± 0.39 | – | – | – |
| | | 5 | – | 8.39 ± 0.55 | – | 108.2 | – |
| | | – | 5 | – | 8.33 ± 0.32 | – | 107.0 |
| | | 10 | – | 12.92 ± 0.23 | – | 99.4 | – |
| | | – | 10 | – | 12.80 ± 0.83 | – | 98.2 |
| Distilled water | | – | – | BLD | – | – | – |
| | | 5 | – | 5.25 ± 0.03 | – | 105.0 | – |
| | | – | 5 | – | 5.54 ± 0.14 | – | 110.8 |
| | | 10 | – | 10.93 ± 0.29 | – | 109.3 | – |
| | | – | 10 | – | 10.39 ± 0.15 | – | 103.9 |

Notes: BLD (below the limit of detection) is 0.5 μg L$^{-1}$. EnviroMAT drinking water lot no: EP-L-2, cataloque no: 140-025-031.

The calibration graphs were obtained with the direct use of As(III) standards and also by measuring the adsorbed arsenic after preconcentration from 50 mL solution to 5 mL (enrichment factor = 10). The results are shown in Fig. 8. No significant differences were observed in the calibrated graphs. Considering that the enrichment factor is 50, the calibration graph can be drawn in the range of 0.1–20 μg $L^{-1}$ As(III).

Limit of detection (3$\sigma$ of the blank) for the direct determination of arsenic was 1.2 μg $L^{-1}$ for the batch method and 0.5 μg $L^{-1}$ for the continuous flow method. With the 50 times preconcentration, the LOD values are 0.024 and 0.010 μg $L^{-1}$ for the batch and continuous flow method, respectively. The relative standard deviations of the batch method and the continuous flow method for the determination of 20 μg $L^{-1}$ As(III) were 4.8% ($n = 7$) and 1.4% ($n = 7$), respectively, for direct measurements. Repeatability of the method using the preconcentration procedure was evaluated by adding 50 mL of 5 μg $L^{-1}$ As(III) solutions at pH ~6 on 10 mg Ni/$Ni_xB$ nanoparticles. The final solution volumes for arsenic measurements were adjusted to 10 mL. The adsorption and recovery procedures were repeated seven times. The relative standard deviation was found to be 3.4% ($n = 7$), with the continuous flow method.

The validation of the presented procedure has been evaluated by the analysis of certified reference material (CRM) (EnviroMAT Drinking water-Low, EP-L-2) employing the adsorption and recovery procedures. The results found were in good agreement with the certified values of CRM and are shown in Table 4.

### 3.12. Application to real samples

The proposed method has been applied to determination of As(III) in tap water, mineral water, and commercially bottled drinking water. The pH of the sample was adjusted to 6.0. Afterward, 25 mL of 5 and 10 μg $L^{-1}$ of As(III) and As(V) spiked tap water and mineral water samples as well as unspiked samples were added individually to 10 mg adsorbent. The mixtures were shaken for an hour for the adsorption, and then, the adsorbent phase and liquid phase were separated by filtration. The adsorbents were dissolved in 5 mL, 2 mol $L^{-1}$ HCl. The results are shown in Table 4. The results indicated that the recoveries were quantitative for trace arsenic analysis, ranging from 99.4 to 112.1%.

## 4. Conclusions

A novel adsorbent abbreviated as Ni/$Ni_xB$ nanoparticles which provides high adsorption efficiency (99.5%), and extremely high capacity for both As(III) and As(V) (2.50 g $g^{-1}$ adsorbent) was introduced. The enrichment ratio was 50. The adsorbent possesses fast adsorption kinetic for both As(III) and As(V). Under the optimized conditions, the overall relative standard deviation for the adsorption and determination of 5 μg $L^{-1}$ As(III) in 50 mL solution was found to be 3.4% ($n = 7$). The method was validated by applying to a CRM drinking water sample and measuring the recoveries of the spiked arsenic to bottled water, tap water, mineral water, and distilled water.

## Acknowledgments

We would like to thank Ege University Research Fund for the financial support of this study, Project No. 2010 FEN 079. Yasemin İşlek Coşkun also thanks the Scientific and Technological Research Council of Turkey (TUBITAK) for scholarship during this study.

## References

[1] C. Xiong, M. He, B. Hu, On-line separation and preconcentration of inorganic arsenic and selenium species in natural water samples with CTAB-modified alkyl silica microcolumn and determination by inductively coupled plasma-optical emission spectrometry, Talanta 76 (2008) 772–779.

[2] D.Q. Hung, O. Nekrassova, R.G. Compton, Analytical methods for inorganic arsenic in water: A review, Talanta 64 (2004) 269–277.

[3] WHO, Arsenic in drinking water, WHO Guidel. Drink. Qual. (2011) 1–24. Available from: <http://www.who.int/water_sanitation_health/dwq/chemicals/arsenic.pdf>.

[4] S. Yamamura, J. Bartram, M. Csanady, H.G. Gorchev, A. Redekopp, Drinking water guidelines and standards, United Nations Synth. Rep. Arsen. Drink. Water (2003) 1–18. Available from <http://www.who.int/water_sanitation_health/dwq/arsenicun5.pdf>.

[5] Marcela Burguera and Jose Luis Burguera, Analytical methodology for speciation of arsenic in environmental and biological samples, Talanta 44 (1997) 1581–1604.

[6] A. Kaur, U. Gupta, A review on applications of nanoparticles for the preconcentration of environmental pollutants, J. Mater. Chem. 19 (2009) 8279–8289.

[7] J. Wang, W. Xu, L. Chen, X. Huang, J. Liu, Preparation and evaluation of magnetic nanoparticles impregnated chitosan beads for arsenic removal from water, Chem. Eng. J. 251 (2014) 25–34.

[8] S. Bhowmick, S. Chakraborty, P. Mondal, W. Van Renterghem, S. Van den Berghe, G. Roman-Ross, D. Chatterjee, M. Iglesias, Montmorillonite-supported nanoscale zero-valent iron for removal of arsenic from aqueous solution: Kinetics and mechanism, Chem. Eng. J. 243 (2014) 14–23.

[9] R. Li, Q. Li, S. Gao, J.K. Shang, Exceptional arsenic adsorption performance of hydrous cerium oxide nanoparticles: Part A. Adsorption capacity and mechanism, Chem. Eng. J. 185–186 (2012) 127–135.

[10] W. Tang, Q. Li, S. Gao, J.K. Shang, Arsenic(III, V) removal from aqueous solution by ultrafine α-$Fe_2O_3$ nanoparticles synthesized from solvent thermal method, J. Hazard. Mater. 192 (2011) 131–138.

[11] H. Erdoğan, Ö. Yalçınkaya, A.R. Türker, Determination of inorganic arsenic species by hydride generation atomic absorption spectrometry in water samples after preconcentration/separation on nano $ZrO_2/B_2O_3$ by solid phase extraction, Desalination 280 (2011) 391–396.

[12] A.Z.M. Badruddoza, Z.B.Z. Shawon, M.T. Rahman, K.W. Hao, K. Hidajat, M.S. Uddin, Ionically modified magnetic nanomaterials for arsenic and chromium removal from water, Chem. Eng. J. 225 (2013) 607–615.

[13] F. Deng, R. Dong, K. Yu, X. Luo, X. Tu, S. Luo, L. Yang, Determination of trace total inorganic arsenic by hydride generation atomic fluorescence spectrometry after solid phase extraction-preconcentration on aluminium hydroxide gel, Microchim. Acta (2013) 509–515.

[14] E. Henden, Y. İşlek, M. Kavas, N. Aksuner, O. Yayayürük, T.D. Çiftçi, R. İlktaç, A study of mechanism of nickel interferences in hydride generation atomic absorption spectrometric determination of arsenic and antimony, Spectrochim. Acta, Part B 66 (2011) 793–798.

[15] T.D. Çiftçi, E. Henden, Nickel/nickel boride nanoparticles coated resin: A novel adsorbent for arsenic(III) and arsenic(V) removal, Powder Technol. 269 (2015) 470–480.

[16] N. Erdem, E. Henden, Inter-element interferences in the determination of arsenic and antimony by hydride generation atomic absorption spectrometry with a quartz tube atomizer, Anal. Chim. Acta 505 (2004) 59–65.

[17] T.D. Çiftçi, O. Yayayürük, E. Henden, Study of arsenic (III) and arsenic(V) removal from waters using ferric hydroxide supported on silica gel prepared at low pH, Environ. Technol. 32 (2011) 341–351.

[18] K. Leopold, M. Foulkes, P.J. Worsfold, Gold-coated silica as a preconcentration phase for the determination of total dissolved mercury in natural waters using atomic fluorescence spectrometry, Anal. Chem. 81 (2009) 3421–3428.

[19] É.M. de Moraes Flores, L.L.C. da Silva, J.S. Barin, A.P.F. Saidelles, R. Zanella, V.L. Dressler, J.N.G. Paniz, Minimization of volatile nitrogen oxides interference in the determination of arsenic by hydride generation atomic absorption spectrometry, Spectrochim. Acta, Part B 56 (2001) 1883–1891.

[20] H. Zhu, Y. Jia, X. Wu, H. Wang, Removal of arsenic from water by supported nano zero-valent iron on activated carbon, J. Hazard. Mater. 172 (2009) 1591–1596.

[21] C. Martinson, K.J. Reddy, Adsorption of arsenic(III) and arsenic(V) by cupric oxide nanoparticles, J. Colloid Interface Sci. 336 (2009) 406–411.

[22] S. Sounderajan, G.K. Kumar, S. Kumar, A.C. Udas, G. Venkateswaran, Characterization of As(V), As(III) by selective reduction/adsorption on palladium nanoparticles in environmental water samples, Talanta 78 (2009) 1122–1128.